The spectrin network as a barrier to lateral diffusion in erythrocytes

A percolation analysis

Michael J. Saxton

*Plant Growth Laboratory, Department of Agronomy and Range Science, University of California, Davis, California 95616; and Laboratory of Chemical Biodynamics, Lawrence Berkeley Laboratory, University of California, Berkeley, California 94720

ABSTRACT The spectrin network on the cytoplasmic surface of an erythrocyte can be modeled as a triangular lattice of spectrin tetramers (Tsuji, A., and S. Ohnishi. 1986. *Biochemistry.* 25:6133–6139). The tetramers act as barriers to protein diffusion, while dissociated dimer pairs, single dimers, and missing tetramers do not. Diffusion in the presence of these barriers is shown to be equivalent to bond percolation on the honeycomb lattice. Monte Carlo calculations for this system then yield the relative diffusion constant of a mobile integral protein as a function of the fraction of spectrin tetramers. At high concentrations of spectrin tetramer, long-range diffusion is blocked, but short-range diffusion is still possible. Monte Carlo calculations yield the average distance over which short-range diffusion can occur, as a function of the fraction of spectrin tetramers. Applications to erythrocyte development and hereditary hemolytic anemia are discussed.

INTRODUCTION

Lateral diffusion in an erythrocyte membrane is strongly influenced by the network of spectrin bound to the erythrocyte. Here I present Monte Carlo calculations based on a model of the effect of this network on lateral diffusion. The calculations show the influence of the integrity of the spectrin network on the diffusion constant for long-range diffusion and on the range of short-range diffusion. The model presented here is applicable to protein diffusion in erythrocytes, but lipid diffusion is not significantly influenced by the presence of spectrin (Sheetz et al., 1980; Bloom and Webb, 1983).

At the cytoplasmic surface of the erythrocyte, spectrin heterodimers are associated end-to-end to form tetramers. Actin and band 4.1 are bound to the other end of the tetramers, linking them into a network. Spectrin is connected to band 3 by ankyrin and to glycophorin by band 4.1. These connections to integral proteins bind the network to the membrane. (Cohen, 1983; Goodman and Shiffer, 1983; Sheetz, 1983; Bennett, 1985; Marchesi, 1985; Anderson, 1986).

Approximately 40% of the band 3 dimer is bound to the spectrin network; the rest is unattached (Nigg and Cherry, 1980). The band 3 molecules bound to spectrin are immobile, showing no rotational or lateral diffusion. The remaining molecules of band 3 show free rotational diffusion (at a rate influenced by the self-association of band 3), but long-range lateral diffusion is blocked by the spectrin network (Cherry et al., 1976; Mühlebach and Cherry, 1985). The length of a spectrin tetramer is ~76 nm in the native conformation, and 200 nm in the fully extended conformation (Sheetz, 1983). If unbound molecules of band 3 are trapped in regions of this size, band 3 is then immobile over the distances of 1 to 2 μm observed in photobleaching experiments.

The influence of the spectrin network on lateral diffusion has been demonstrated in many experiments in which agents altering the structure of the network have a major effect on the lateral diffusion of integral proteins. Addition of ankyrin decreases the amount of band 3 that is mobile but does not change the diffusion constant of the mobile fraction (Tsuji and Ohnishi, 1986). Blocking the connection between spectrin and band 3 by adding the 72-kD fragment of ankyrin increases the diffusion rate of integral proteins (Fowler and Bennett, 1978; Golan and Veatch, 1982). Removal of the cytoplasmic domain of band 3 by treatment with trypsin increases the diffusion constant of band 3 by a factor of 8 (Tsuji and Ohnishi, 1986). Polyphosphates disrupt the spectrin–actin linkage and increase the diffusion constant of integral protein (Schindler et al., 1980; Sheetz et al., 1982; Tsuji and Ohnishi, 1986). Polyamines decrease the diffusion constant, either by binding polyphosphates or by interacting with membrane proteins directly (Schindler et al., 1980; Tsuji and Ohnishi, 1986). Diamide crosslinks spectrin and decreases the mobility of band 3 (Smith and Palek, 1982). Low temperatures and high ionic strength increase spectrin association and lower the diffusion constant (Golan and Veatch, 1980). In spherocytic mouse cells, spectrin is absent, and the diffusion rate of integral proteins is ≈50 times that observed in normal cells (Sheetz et al., 1980). In tethers, the lipid bilayer is separated from the membrane skeleton, and lateral diffusion is greatly enhanced (Berk et al., 1988).

In early work, spectrin was simply thought of as a network of unspecified geometry (Steck, 1974; Cherry et al., 1976). Sheetz (1983) pictured the network as a

0006-3495/89/01/21/08 $2.00

latticework of corrals with gates that are open or closed depending on the association of the spectrin tetramers. Recent electron microscopy has shown that in spread erythrocytes 80 to 90% of the spectrin is organized into a triangular lattice (Beaven et al., 1985; Byers and Branton, 1985; and especially Liu et al., 1987). Not all junctions have exactly six spectrin molecules attached, and higher oligomers of spectrin may be present in low concentrations, but on the average the structure is well represented by a triangular lattice.

Assume a model in which the spectrin network forms a triangular lattice, as shown in Fig. 1 *a*. The junctions consist of actin and band 4.1. All adjacent junctions are potentially connected by spectrin tetramers. Tetramers act as barriers to protein diffusion, while dissociated dimer pairs, single dimers, and missing tetramers allow proteins to diffuse from triangle to adjacent triangle. This model is a slight generalization of that of Tsuji and Ohnishi (1986).

Label the interior of each triangle with an open circle, representing the average position of a free integral protein in the triangle, and observe that the open circles form a honeycomb lattice (Fig. 1 *b*). Then connect neighboring open circles by bonds. A spectrin tetramer corresponds to a blocked bond, and a dissociated dimer pair corresponds to a conducting bond (Fig. 1 *c*). Thus, long-range diffusion through the spectrin network is equivalent to bond percolation on the honeycomb lattice, which is the dual of the triangular lattice (Wannier, 1945). If the lattice constant in the triangular lattice is l_{TRI}, then the lattice constant in the honeycomb lattice is $l_{HC} = l_{TRI}/\sqrt{3}$. (An excellent introduction to percolation theory is given by Stauffer [1985]; applications to lateral diffusion are discussed by Saxton [1982, 1987*b*].)

Since diffusion through the spectrin network is equivalent to diffusion on a lattice, a percolation threshold exists. At concentrations of blocked bonds below the threshold, diffusion is possible over an arbitrarily long range; above the threshold, long-range diffusion is blocked. Only short-range diffusion is possible, and the range of short-range diffusion decreases as the concentration of blocked bonds increases.

Consider the following analogy. Suppose that one is trying to cross a town, and the public works department is barricading the streets at random. Long before every street is barricaded, it will be impossible to travel across town, though travel in small neighborhoods will still be possible. Bond percolation corresponds to barricades in the middle of blocks; site percolation, to barricades of intersections. The lowest fraction of random barricades sufficient to prevent long-range travel corresponds to the percolation threshold.

Bond percolation on a lattice can be treated readily by Monte Carlo techniques. A lattice is constructed with a prescribed fraction of the bonds blocked at random. Then a tracer particle is placed at random at a lattice site and allowed to move by a random walk for a prescribed number of time steps. This calculation is repeated for an ensemble of tracers and lattice configurations, and the mean-square displacement is found as a function of the number of time steps. The diffusion constant is obtained from the mean-square displacement. These calculations yield the diffusion constant as a function of the fraction of bonds blocked. This treatment is appropriate when each bond remains open or closed over the entire course of the diffusion measurement; the case of transient barriers is discussed below.

METHODS

The general approach to Monte Carlo calculations of lattice diffusion is similar to that used earlier (Saxton, 1987*b*). To treat bond percolation, extensive modification to the program was required.

The algorithm used is as follows. First, a linked list is constructed for the perfect honeycomb lattice, listing all the sites and the sites to which they are connected. Then, a random site and a random bond at that site are chosen and blocked; this is repeated until the prescribed fraction of bonds has been blocked. Next, a random site is chosen as the starting

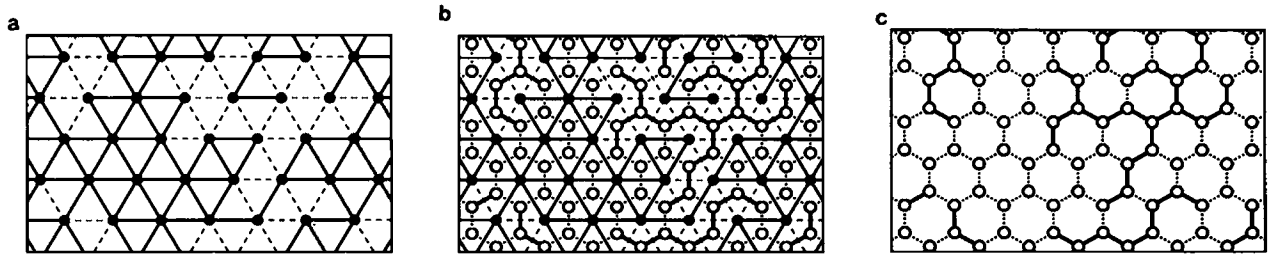

FIGURE 1 Geometry of the spectrin lattice and the resulting bond percolation model. (*a*) Triangular lattice of junctions connected by spectrin tetramers (*solid line*) or dissociated dimer pairs (*dashed line*) as in the model of Tsuji and Ohnishi (1986). (*b*) The same lattice with interiors of triangles marked by open circles, forming a honeycomb lattice. (*c*) The honeycomb lattice derived from *a*. Paths obstructed by tetramers in *a* correspond to blocked bonds in *b* and *c* (*dashed lines*); unblocked paths in *a* correspond to conducting bonds in *b* and *c* (*solid lines*).

point of the tracer executing the random walk. At each time step of the random walk, one of the three bonds at the current location of the tracer is chosen at random. If the bond is conducting, the tracer is moved to the appropriate site; if the bond is blocked, the tracer is not moved. In either case the time is increased by one unit. This procedure is repeated for a fixed number of time steps, and the position of the tracer is recorded periodically. The random walk is repeated for various starting points within a fixed configuration of blocked bonds, and for various configurations of blocked bonds. These calculations yield the mean-square displacement $\langle r^2 \rangle$ of the ensemble of tracers as a function of time t for a given fraction b of blocked bonds. Below the percolation threshold, this is fit to the equation

$$\langle r^2(t) \rangle = 4Dt + A + B \ln t \qquad (1)$$

as described previously (Saxton, 1987*b*), and the normalized diffusion constant

$$D^*(b) = D(b)/D(0) \qquad (2)$$

is evaluated. Here $D(0) = \Gamma l_{HC}^2/4$ is the diffusion constant for the perfect lattice, l_{HC} is the lattice constant, and Γ is the jump rate of tracers, here taken to be the reciprocal of the unit of time. The terms $A + B \ln t$ in Eq. 1 come from the long-time tail in the velocity autocorrelation function (Tahir-Kheli and El-Meshad, 1985; Van Beijeren and Kutner, 1985). These terms lower the diffusion constant by 1% or less for $b \leq 0.20$, 10% or less for $0.25 \leq b \leq 0.325$, and 30% for $b = 0.345$, near the percolation threshold.

The calculations were carried out for a 201 × 201 lattice with periodic boundary conditions. Typically, in the calculations of $D^*(b)$ below the percolation threshold, 150,000 time steps were used for each of 50 configurations of bonds and 100 tracers per bond configuration. If necessary, longer runs (300,000 time steps) were used to evaluate $\langle r^2(\infty) \rangle$.

RESULTS

The diffusion constant as a function of spectrin tetramer concentration

Results of the Monte Carlo calculations are presented in Fig. 2, which shows the mean-square displacement $\langle r^2 \rangle$ as a function of time for various fractions b of blocked bonds. Below the percolation threshold, for large times, $\langle r^2 \rangle$ increases linearly with time, and the diffusion constant is obtained from the asymptotic slope according to Eq. 1. Above the percolation threshold, diffusing particles are trapped in small clusters, and $\langle r^2(t) \rangle$ reaches a finite limit $\langle r^2(\infty) \rangle$, proportional to the average size of a cluster of connected bonds at that concentration.

In Fig. 3, the normalized diffusion constant $D^*(b)$ is given as a function of the fraction b of blocked bonds (corresponding to the fraction of spectrin present as tetramers or higher oligomers. All of these are counted as tetramers). Fig. 3 also shows the effective-medium approximation (Kirkpatrick, 1973) for the percolation

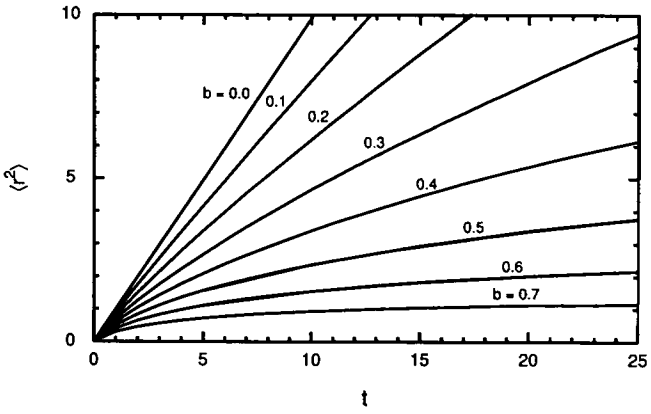

FIGURE 2 Mean-square displacement $\langle r^2 \rangle$ of diffusing particles as a function of time for diffusion on the honeycomb lattice with various fractions b of blocked bonds. The unit of length is the lattice spacing l_{HC}, and the unit of time is the reciprocal of the jump frequency Γ.

curve:

$$D^*(b) = 1 - 3b. \qquad (3)$$

Eq. 3 is a good approximation except in the neighborhood of b_c, accurate to 10% or better for $b \leq 0.30$.

As shown in Fig. 3, the diffusion constant decreases monotonically with the fraction of tetramers, and goes to zero at the theoretically established percolation threshold $b_c = 0.34729$ (Essam, 1972). (In the percolation literature, the percolation threshold is usually given in terms of the fraction of conducting bonds p_c, not the fraction of blocked bonds b_c, so $b_c = 1 - p_c$.) In normal erythrocytes, $b = 0.95$ (see below), so that long-range diffusion, as

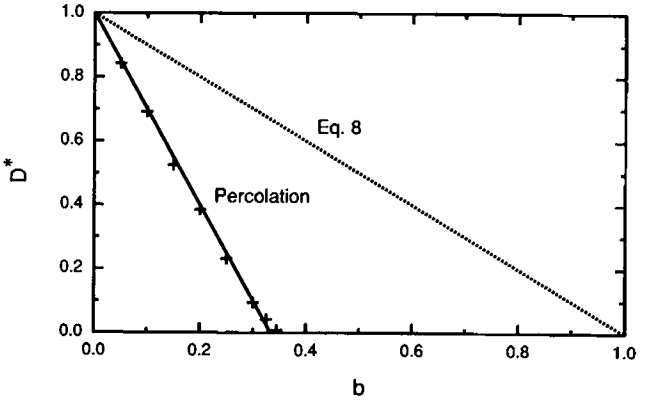

FIGURE 3 Normalized diffusion constant D^* as a function of the fraction b of blocked bonds. The percolation curve is applicable when the barrier lifetime is long on the time scale of the measurement; Eq. 8, when the barrier lifetime is short. *Crosses*, data points from Monte Carlo calculations. *Dotted line*, Eq. 8. *Solid line*, Eq. 3, the effective-medium approximation to the percolation curve.

measured in fluorescence photobleaching experiments, is blocked. Experiment shows that the diffusion constant of band 3 in normal erythrocytes is $\approx 1/400$ that of band 3 reconstituted in dimyristoylphosphatidylcholine (Chang et al., 1981).

To choose the reference state $D(0)$ in Eq. 2 appropriately, we must examine the effects of various classes of proteins on lateral diffusion. Consider a lipid bilayer with the composition and asymmetry of the erythrocyte bilayer. If band 3 and glycophorin were added to the bilayer at physiological concentrations, the diffusion constants of lipid and protein would be lowered (Saxton, 1982; Golan et al., 1984). The diffusion constant of band 3 in such a membrane is equivalent to that measured by Sheetz et al. (1980) in erythrocytes of spherocytic (S^-) mice, for which $D(S^-) = 250 \times 10^{-11}$ cm^2/s. If spectrin dimer, actin, and the other proteins of the membrane skeleton were then bound to the bilayer at physiological concentrations, the diffusion constant would be lowered further, to a value D(dimer). If the spectrin were then allowed to form tetramers, the diffusion constant would be lowered to a value D(normal) $= 4 \times 10^{-11}$ cm^2/s (Golan and Veatch, 1980; Sheetz et al., 1980; Chang et al., 1981; Koppel et al., 1981).

If measurements are made on cells in which part of the spectrin is missing, the appropriate reference state is $D(S^-)$, the value with no spectrin present. If spectrin is present at normal concentration but unable to associate normally, the appropriate reference state is D(dimer).

The range of short-range diffusion

Above the percolation threshold, only short-range diffusion is possible, but percolation effects are still observable. Fig. 2 shows that as the concentration of blocked bonds increases, a diffusing particle is restricted to smaller and smaller neighborhoods, until finally it is trapped in a single triangle of the spectrin lattice.

The distance over which short-range diffusion can occur can be related to b by percolation theory (Stauffer, 1985). Near the percolation threshold b_c,

$$\langle r^2(\infty) \rangle = A_0 \epsilon^{\beta - 2\nu}, \quad (4)$$

where $\epsilon = |b - b_c|$ is the distance from the percolation threshold, β and ν are scaling exponents, and A_0 is a constant. (The exponent ν describes the scaling behavior of the correlation length ξ, an average cluster size: $\xi \sim \epsilon^{-\nu}$. The exponent β comes from averaging over all cluster sizes.) The scaling exponents are $\beta = 5/36$ and $\nu = 4/3$ (Stauffer, 1985), and A_0 is evaluated from a least-square fit to the Monte Carlo results, giving

$$\langle r^2(\infty) \rangle = 0.0991(b - b_c)^{-2.5278}. \quad (5)$$

Fig. 4 shows values of $\langle r^2(\infty) \rangle$ from the Monte Carlo calculations and from Eq. 5. The scaling law breaks down far from the percolation threshold, but this is of little practical importance. A tracer is always free to diffuse within its own triangle of spectrin tetramers, so that, as shown in Fig. 4, $\langle r^2(\infty) \rangle$ can be no smaller than $\frac{1}{6} l_{TRI}^2 = \frac{1}{2} l_{HC}^2$, twice the radius of gyration (Mitescu and Rousseng, 1983; Vicsek, 1983) of an equilateral triangle of side l_{TRI}. In Eq. 5, $\langle r^2(\infty) \rangle$ is expressed in lattice constants for the honeycomb lattice, $l_{HC} = 44$ nm. So in the normal membrane, with 5% dimer, the diffusion distance $\langle r^2(\infty) \rangle$ is 690 nm^2. In a pathological erythrocyte (see below) with 36% dimer (Liu et al., 1981), $b = 0.64$, and $\langle r^2(\infty) \rangle = 4{,}300$ nm^2.

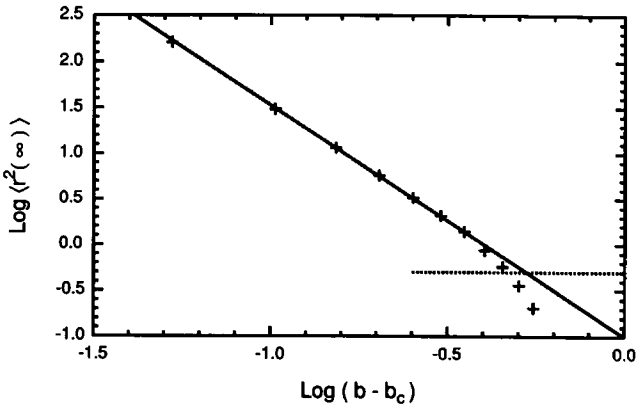

FIGURE 4 Double logarithmic plot of limiting cluster size $\langle r^2(\infty) \rangle$ as a function of the distance $b - b_c$ from the percolation threshold $b_c = 0.34729$. The unit of length is the lattice spacing l_{HC}. *Crosses*, data points from Monte Carlo calculations. *Solid line*, Eq. 5. *Dotted line*, limiting value $\frac{1}{2} l_{HC}^2$.

The diffusion constant calculated in this paper is the value for long-range diffusion. As shown by Eisinger et al. (1986), in the presence of obstacles the short-range and long-range diffusion constants are different. The dependence of the diffusion constant on the distance over which diffusion is measured can be obtained from Monte Carlo calculations (Saxton, 1987*a*).

DISCUSSION

Changes in the membrane skeleton during development

Concanavalin A induces clustering and endocytosis of its binding sites in neonatal erythrocytes but not in adult erythrocytes, as demonstrated by electron microscopy. Small clusters are formed, but capping does not occur, suggesting that membrane proteins are mobile in discrete domains (Schekman and Singer, 1976). The clustering occurs in regions free from spectrin, as shown in experi-

ments in which cells pretreated with concanavalin A were labeled with a ferritin-labeled antibody to spectrin. Invaginations and intracellular vesicles showed no labeling for spectrin, while areas of membrane adjacent to invaginations were heavily labeled (Tokuyasu et al., 1979). Similarly, concanavalin A–induced endocytosis decreases during maturation of reticulocytes. This was attributed to the progressive elimination of gaps in the spectrin network (Zweig and Singer, 1979). Both endocytotic and exocytotic vesicles are depleted in spectrin and actin (Schrier et al., 1986, and references cited therein).

These results can be understood in terms of the percolation model. As spectrin is added to the network, the long-range diffusion constant decreases as shown in the percolation curve in Fig. 3. At the percolation threshold, long-range diffusion is blocked, and further addition of spectrin reduces the distance over which short-range diffusion can occur, as shown in Fig. 4.

Abnormalities in the spectrin network

Abnormalities in the spectrin network can result from a deficiency of normal protein, or from various defects in the proteins preventing normal protein–protein association (Palek and Lux, 1983; Becker and Lux, 1985; Palek, 1985; Zail, 1986). Abnormalities affecting individual spectrin linkages in an uncorrelated manner are equivalent: the absence of spectrin, defects in spectrin–spectrin binding, the absence of band 4.1, or defects in spectrin–band 4.1 binding. These defects simply decrease the fraction b of tetramers. A qualitatively different problem would result from a defect in actin preventing normal binding of spectrin. In this case, a junction in the triangular lattice is removed, not a bond, so that all six bonds surrounding that junction are absent, and the corresponding six bonds in the dual honeycomb lattice are unblocked. This is a correlated bond percolation problem, with a different percolation threshold from the usual uncorrelated problem.

An abnormal erythrocyte can have both a deficiency of spectrin and a defect blocking dimer–dimer association. The fraction b of tetramer can be obtained from measurable quantities as follows. Let F_M be the fraction of spectrin missing. The observed ratio of spectrin to band 3 in a ghost is then $1 - F_M$. If n_D moles of dimer and n_T moles of tetramer are bound to the membrane, then the mole fraction of dimer unable to associate normally is simply the observed fraction of spectrin dimer, $F_D = n_D/(n_D + 2n_T)$. (This quantity is measured by nondenaturing gel electrophoresis at low temperature [Palek, 1985].) Then

$$b = 1 - [F_M + (1 - F_M)F_D]. \quad (6)$$

The first term in the brackets represents the missing spectrin, and the second term represents spectrin that is present but unable to associate normally. So

$$b = (1 - F_M)(1 - F_D). \quad (7)$$

The concentration of dimer is well below the percolation threshold in normal erythrocytes and in most cases of hereditary hemolytic anemia. In normal erythrocytes, the fraction of dimers is approximately 5% (Palek and Lux, 1983), and $b = 0.95$. Eight cases of hereditary elliptocytosis showed 15 to 33% dimer (Liu et al., 1982), giving $b = 0.67$ to 0.85. Liu et al. (1981) reported two cases of hereditary pyropoikilocytosis with 30 to 40% dimer, so that $b = 0.6$ to 0.7. Agre et al. (1985) reported a case of hereditary spherocytosis in which the spectrin/band 3 ratio is 0.45 by radioimmunoassay, so that $b = 0.45$. Rarely, the dimer concentration is above the percolation threshold. In one case of hereditary pyropoikilocytosis (Peterson et al., 1987), only 69% of the normal amount of spectrin is present, and of the spectrin that is present 61% is dimer, so that $b = 0.27$. In a case of homozygous hereditary elliptocytosis (Evans et al., 1983), there was 82% dimer, and $b = 0.18$, apparently the lowest value that has been found in human erythrocytes. Mouse spherocytes have been reported in which all the spectrin is missing (Greenquist et al., 1978; Shohet, 1979). Very low concentrations of spectrin are uncommon; if the concentrations of spectrin are low enough to allow diffusion, the erythrocytes are very fragile. This behavior would be predicted by a percolation model of elasticity (for example, Kantor and Webman, 1984; Sahimi and Goddard, 1986).

Transient barriers

The percolation curve in Fig. 3 is appropriate when the bonds remain open or closed over the entire course of a diffusion measurement. The straight line in Fig. 3 is the limit in which the bonds open and close so quickly that there is no correlation between one attempt of a tracer to move and the next. A tracer attempting to move to an adjacent site is blocked with a probability b and is successful with a probability $1 - b$. The diffusion constant is simply

$$D^*(b) = 1 - b, \quad (8)$$

and there is no percolation threshold. Intermediate rates of bond opening are expected to yield intermediate curves, just as in the site problem with mobile obstacles on the square lattice (Saxton, 1987*b*) and the triangular lattice (Saxton, 1988).

Tsuji and Ohnishi (1986) measured the diffusion constant of band 3 as a function of dimer concentration over

the range $b = 0.50$ to 0.67. The observed diffusion constants yield $D^* = 0.021$ to 0.0016, while the percolation model predicts that the diffusion constant is zero for this range of b. These results suggest that the actual diffusion constant follows an intermediate curve that is close to the percolation curve but does not have such a sharp cutoff at the percolation threshold. A curve of this form would be expected if the time for barriers to open and close was somewhat shorter than the characteristic time for the photobleaching measurement. (In these experiments, the beam radius r was 0.8 μm, so that the characteristic diffusion time is $\tau = r^2/4D = 40$ s.)

If spectrin is unable to associate normally, as in cells with defective spectrin or in normal cells treated with a sulfhydryl-blocking agent (Smith and Palek, 1983), the observed diffusion constant will follow this modified percolation curve. If agents are used which increase the rate of breaking and reforming tetramers, such as 2,3-diphosphoglycerate (Sheetz, 1983), $D^*(c)$ will be shifted toward the curve of Eq. 8, and the cutoff at the percolation threshold will be less distinct.

Koppel et al. (1981) presented a model of matrix control of diffusion in which diffusion involves two independent events: (a) Free diffusion between barriers at a rate determined by the bilayer (diffusion constant D_{BL}); and (b) breakdown and crossing of the barrier (diffusion constant D_M). The overall diffusion constant is then $D = D_{BL}D_M/(D_{BL} + D_M)$. Following Koppel et al. (1981), assume that $D_M = \lambda^2/4\tau$. Here the average area per barrier is λ^2, and the diffusion time is $\tau = \tau_{CL}/P$, where τ_{CL} is the average length of time a barrier is closed, and P is the probability that the particle will cross an open barrier. For the lattice geometry assumed here,

$$\lambda^2 = \sqrt{3}l_{HC}^2/2b, \tag{9}$$

so that

$$D_M = \sqrt{3}Pl_{HC}^2/8b\tau_{CL}. \tag{10}$$

Consider the limit in which barrier crossings are rate-limiting, so that $D = D_M$. In Eq. 10, take $P = 1$, $b = 1$, $l_{HC} = 44$ nm, and $D = 4 \times 10^{-11}$ cm^2/s. Then $\tau_{CL} = 0.1$ s. That is, for diffusion to occur at the observed rate, the barriers have to open every 0.1 s.

For spectrin in solution, the kinetic measurements of Ungewickell and Gratzer (1978) give an opening rate of 1.6×10^{-3} s^{-1}, so that $\tau_{CL} = 625$ s. The large discrepancy between the calculated and observed values of τ_{CL} would be resolved if the rate of dimer–tetramer conversion in the erythrocyte is much higher than that observed in solution (Sheetz and Casaly, 1981; Sheetz, 1983). The conversion rates may differ because binding of spectrin to the erythrocyte membrane increases the local concentration of spectrin and constrains its geometry (Liu and Palek, 1980), or because the concentration of 2,3-diphosphoglycerate and the ionic strength are different in solution and in the erythrocyte (see Sheetz and Casaly, 1981; Sheetz, 1983; Waugh, 1986.) Alternatively, the conformational change permitting crossing of the spectrin barrier is something other than tetramer–dimer conversion, such as the transient detachment of a segment of the spectrin tetramer from the membrane.

An alternative to the barrier model is one in which protein diffusion is slowed by transient low-affinity binding of mobile species to immobile species of the membrane skeleton. Sheetz (1983) discusses the two models and argues that the barrier effect predominates. But both effects could occur simultaneously; band 3 is known to self-associate (Mühlebach and Cherry, 1985).

Applicability to other cells

Spectrin-like molecules form networks associated with the plasma membrane in a wide variety of cells other than erythrocytes (Nelson and Lazarides, 1984; Pauly et al., 1986; Goodman and Zagon, 1986; Nelson and Veshnock, 1986). The treatment presented here is qualitatively applicable to these cells. Other network geometries will yield similar curves for $D^*(b)$, but the percolation threshold will depend on the coordination number z of the lattice. Values of the percolation threshold range from 0.35 for the honeycomb lattice ($z = 3$) to 0.65 for the triangular lattice ($z = 6$) (Stauffer, 1985).

I thank M. P. Klein and R. W. Breidenbach for their encouragement of this research, L. Zondek for his inspiration, the reviewers for their comments, and Sun Un for the use of his graphics programs. Computer time was generously provided by the Laboratory of Chemical Biodynamics.

This research was supported in part by National Institutes of Health grant 1 R01 GM38133-01A1.

Received for publication 15 April 1988 and in final form 19 August 1988.

REFERENCES

Agre, P., J. F. Casella, W. H. Zinkham, C. McMillan, and V. Bennett. 1985. Partial deficiency of erythrocyte spectrin in hereditary spherocytosis. *Nature (Lond.)*. 314:380–383.

Anderson, R. A. 1986. Glycophorin-protein 4.1: a transmembrane protein complex that may regulate the erythrocyte membrane skeleton. *In* Membrane Skeletons and Cytoskeletal-Membrane Associations. V. Bennett, C. M. Cohen, S. E. Lux, and J. Palek, editors. Alan R. Liss, Inc., New York. 223–241.

Beaven, G. H., L. Jean-Baptiste, E. Ungewickell, A. J. Baines, F. Shahbakhti, J. C. Pinder, S. E. Lux, and W. B. Gratzer. 1985. An examination of the soluble oligomeric complexes extracted from the

red cell membrane and their relation to the membrane cytoskeleton. *Eur. J. Cell Biol.* 36:299–306.

Becker, P. S., and S. E. Lux. 1985. Hereditary spherocytosis and related disorders. *Clin. Haematol.* 14 (No. 1):15–43.

Bennett, V. 1985. The membrane skeleton of human erythrocytes and its implications for more complex cells. *Annu. Rev. Biochem.* 54:273–304.

Berk, D. A., A. Clark, Jr., and R. M. Hochmuth. 1988. Extensional failure of red cell membrane enhances the lateral mobility of integral proteins. *Biophys. J.* 53 (2, Pt. 2):496a. (Abstr.)

Bloom, J. A., and W. W. Webb. 1983. Lipid diffusibility in the intact erythrocyte membrane. *Biophys. J.* 42:295–305.

Byers, T. J., and D. Branton. 1985. Visualization of the protein associations in the erythrocyte membrane skeleton. *Proc. Natl. Acad. Sci. USA.* 82:6153–6157.

Chang, C.-H., H. Takeuchi, T. Ito, K. Machida, and S. Ohnishi. 1981. Lateral mobility of erythrocyte membrane proteins studied by the fluorescence photobleaching recovery technique. *J. Biochem.* 90:997–1004.

Cherry, R. J., A. Bürkli, M. Busslinger, G. Schneider, and G. R. Parish. 1976. Rotational diffusion of band 3 proteins in the human erythrocyte membrane. *Nature (Lond.).* 263:389–393.

Cohen, C. M. 1983. The molecular organization of the red cell membrane skeleton. *Semin. Hematol.* 20:141–158.

Eisinger, J., J. Flores, and W. P. Petersen. 1986. A milling crowd model for local and long-range obstructed lateral diffusion: mobility of excimeric probes in the membrane of intact erythrocytes. *Biophys. J.* 49:987–1001.

Essam, J. W. 1972. Percolation and cluster size. *In* Phase Transitions and Critical Phenomena, Vol. 2. C. Domb and M. S. Green, editors. Academic Press, London and New York. 197–270.

Evans, J. P. M., A. J. Baines, I. M. Hann, I. Al-Hakim, S. M. Knowles, and A. V. Hoffbrand. 1983. Defective spectrin dimer-dimer association in a family with transfusion dependent homozygous hereditary elliptocytosis. *Br. J. Haematol.* 54:163–172.

Fowler, V., and V. Bennett. 1978. Association of spectrin with its membrane attachment site restricts lateral mobility of human erythrocyte integral membrane proteins. *J. Supramol. Struct.* 8:215–221.

Golan, D. E., and W. Veatch. 1980. Lateral mobility of band 3 in the human erythrocyte membrane studied by fluorescence photobleaching recovery: evidence for control by cytoskeletal interactions. *Proc. Natl. Acad. Sci. USA.* 77:2537–2541.

Golan, D. E., and W. R. Veatch. 1982. Lateral mobility of band 3 in the human erythrocyte membrane: control by ankyrin-mediated interactions. *Biophys. J.* 37(2, Pt. 2):177a. (Abstr.)

Golan, D. E., M. R. Alecio, W. R. Veatch, and R. R. Rando. 1984. Lateral mobility of phospholipid and cholesterol in the human erythrocyte membrane: effects of protein-lipid interactions. *Biochemistry.* 23:332–339.

Goodman, S. R., and K. Shiffer. 1983. The spectrin membrane skeleton of normal and abnormal human erythrocytes: a review. *Am. J. Physiol.* 244 (*Cell Physiol.* 13):C121-C141.

Goodman, S. R., and I. S. Zagon. 1986. The neural cell spectrin skeleton: a review. *Am. J. Physiol.* 250 (*Cell Physiol.* 19):C347-C360.

Greenquist, A. C., S. B. Shohet, and S. E. Bernstein. 1978. Marked reduction of spectrin in hereditary spherocytosis in the common house mouse. *Blood.* 51:1149–1155.

Kantor, Y., and I. Webman. 1984. Elastic properties of random percolating systems. *Phys. Rev. Lett.* 52:1891–1894.

Kirkpatrick, S. 1973. Percolation and conduction. *Rev. Mod. Phys.* 45:574–588.

Koppel, D. E., M. P. Sheetz, and M. Schindler. 1981. Matrix control of protein diffusion in biological membranes. *Proc. Natl. Acad. Sci. USA.* 78:3576–3580.

Liu, S. C., and J. Palek. 1980. Spectrin tetramer-dimer equilibrium and the stability of erythrocyte membrane skeletons. *Nature (Lond.).* 285:586–588.

Liu, S. C., J. Palek, J. Prchal, and R. P. Castleberry. 1981. Altered spectrin dimer-dimer association and instability of erythrocyte membrane skeletons in hereditary pyropoikilocytosis. *J. Clin. Invest.* 68:597–605.

Liu, S. C., J. Palek, and J. T. Prchal. 1982. Defective spectrin dimer-dimer association in hereditary elliptocytosis. *Proc. Natl. Acad. Sci. USA.* 79:2072–2076.

Liu, S. C., L. H. Derick, and J. Palek. 1987. Visualization of the hexagonal lattice in the erythrocyte membrane skeleton. *J. Cell Biol.* 104:527–536.

Marchesi, V. T. 1985. Stabilizing infrastructure of cell membranes. *Annu. Rev. Cell Biol.* 1:531–561.

Mitescu, C. D., and J. Roussenq. 1983. Diffusion on percolation clusters. *Ann. Israel Phys. Soc.* 5:81–100.

Mühlebach, T., and R. J. Cherry. 1985. Rotational diffusion and self-association of band 3 in reconstituted lipid vesicles. *Biochemistry.* 24:975–983.

Nelson, W. J., and E. Lazarides. 1984. Assembly and establishment of membrane-cytoskeleton domains during differentiation: spectrin as a model system. *In* Cell Membranes: Methods and Reviews, Vol. 2. E. Elson, W. Frazier, and L. Glazer, editors. Plenum Publishing Corp., New York. 219–246.

Nelson, W. J., and P. J. Veshnock. 1986. Dynamics of membrane-skeleton (fodrin) organization during development of polarity in Madin-Darby canine kidney epithelial cells. *J. Cell Biol.* 103:1751–1765.

Nigg, E. A., and R. J. Cherry. 1980. Anchorage of a band 3 population at the erythrocyte cytoplasmic membrane surface: protein rotational diffusion measurements. *Proc. Natl. Acad. Sci. USA.* 77:4702–4706.

Palek, J., 1985. Hereditary elliptocytosis and related disorders. *Clin. Haematol.* 14 (No. 1):45–87.

Palek, J., and S. E. Lux. 1983. Red cell membrane skeletal defects in hereditary and acquired hemolytic anemias. *Semin. Hematol.* 20:189–224.

Pauly, J. L., R. B. Bankert, and E. A. Repasky. 1986. Immunofluorescent patterns of spectrin in lymphocyte cell lines. *J. Immunol.* 136:246–253.

Peterson, L. C., C. Dampier, T. Coetzer, J. Lawler, J. White, and J. Palek. 1987. Clinical and laboratory study of two Caucasian families with hereditary pyropoikilocytosis and hereditary elliptocytosis. *Am. J. Clin. Pathol.* 88:58–65.

Sahimi, M., and J. D. Goddard. 1986. Elastic percolation models for cohesive mechanical failure in heterogeneous systems. *Phys. Rev. B.* 33:7848–7851.

Saxton, M. J. 1982. Lateral diffusion in an archipelago: effects of impermeable patches on diffusion in a cell membrane. *Biophys. J.* 39:165–173.

Saxton, M. J. 1987*a*. Lateral diffusion in an archipelago: the distance dependence of the diffusion constant. *Biophys. J.* 51(2, Pt. 2):542a. (Abstr.)

Saxton, M. J. 1987*b*. Lateral diffusion in an archipelago: the effect of mobile obstacles. *Biophys. J.* 52:989–997.

Saxton, M. J. 1988. Lateral diffusion in an archipelago: the effect of large mobile obstacles. *Biophys. J.* 53(2, Pt. 2):510a. (Abstr.)

Schekman, R., and S. J. Singer. 1976. Clustering and endocytosis of membrane receptors can be induced in mature erythrocytes of neonatal but not adult humans. *Proc. Natl. Acad. Sci. USA.* 73:4075–4079.

Schindler, M., D. E. Koppel, and M. P. Sheetz. 1980. Modulation of membrane protein lateral mobility by polyphosphates and polyamines. *Proc. Natl. Acad. Sci. USA.* 77:1457–1461.

Schrier, S. L., I. Junga, and L. Ma. 1986. Endo- and exovesiculation and the structure of the human red cell membrane. *J. Lab. Clin. Med.* 108:265–271.

Sheetz, M. P. 1983. Membrane skeletal dynamics: role in modulation of red cell deformability, mobility of transmembrane proteins, and shape. *Semin. Hematol.* 20:175–188.

Sheetz, M. P., and J. Casaly. 1981. Phosphate metabolite regulation of spectrin interactions. *Scand. J. Clin. Lab. Invest.* 41 (Suppl. 156):117–122.

Sheetz, M. P., M. Schindler, and D. E. Koppel. 1980. Lateral mobility of integral membrane proteins is increased in spherocytic erythrocytes. *Nature (Lond.).* 285:510–512.

Sheetz, M. P., P. Febbroriello, and D. E. Koppel. 1982. Triphosphoinositide increases glycoprotein lateral mobility in erythrocyte membranes. *Nature (Lond.).* 296:91–93.

Shohet, S. B. 1979. Reconstitution of spectrin-deficient, spherocytic mouse erythrocyte membranes. *J. Clin. Invest.* 64:483–494.

Smith, D. K., and J. Palek. 1982. Modulation of lateral mobility of band 3 in the red cell membrane by oxidative cross-linking of spectrin. *Nature (Lond.).* 297:424–425.

Smith, D. K., and J. Palek. 1983. Sulfhydryl reagents induce altered spectrin self-association, skeletal instability, and increased thermal sensitivity of red cells. *Blood.* 62:1190–1196.

Stauffer, D. 1985. Introduction to Percolation Theory. Taylor & Francis, London and Philadelphia.

Steck, T. L. 1974. The organization of proteins in the human red blood cell membrane. *J. Cell Biol.* 62:1–19.

Tahir-Kheli, R. A., and N. El-Meshad. 1985. Correlated diffusion in two-dimensional systems. *Phys. Rev. B.* 32:6166–6175.

Tokuyasu, K. T., R. Schekman, and S. J. Singer. 1979. Domains of receptor mobility and endocytosis in the membranes of neonatal human erythrocytes and reticulocytes are deficient in spectrin. *J. Cell Biol.* 80:481–486.

Tsuji, A., and S. Ohnishi. 1986. Restriction of the lateral motion of band 3 in the erythrocyte membrane by the cytoskeletal network: dependence on spectrin association state. *Biochemistry.* 25:6133–6139.

Ungewickell, E., and W. Gratzer. 1978. Self-association of human spectrin: a thermodynamic and kinetic study. *Eur. J. Biochem.* 88:379–385.

Van Beijeren, H., and R. Kutner. 1985. Mean square displacement of a tracer particle in a hard-core lattice gas. *Phys. Rev. Lett.* 55:238–241.

Vicsek, T. 1983. On random walks in percolation models. *J. Phys. A.* 16:1215–1220.

Wannier, G. H. 1945. The statistical problem in cooperative phenomena. *Rev. Mod. Phys.* 17:50–60.

Waugh, R. E. 1986. Effects of 2,3-diphosphoglycerate on the mechanical properties of erythrocyte membrane. *Blood.* 68:231–238.

Zail, S. 1986. Clinical disorders of the red cell membrane skeleton. *CRC Crit. Rev. Oncol. Hematol.* 5:397–453.

Zweig, S., and S. J. Singer. 1979. Concanavalin A-induced endocytosis in rabbit reticulocytes, and its decrease with reticulocyte maturation. *J. Cell Biol.* 80:487–491.